



Massive phenotyping of multiple cranberry populations reveals novel QTLs for fruit anthocyanin content and other important chemical traits

Luis Diaz-Garcia^{1,2} · Brandon Schlautman³ · Giovanni Covarrubias-Pazaran⁴ · Andrew Maule¹ · Jennifer Johnson-Cicalese⁵ · Edward Grygleski⁶ · Nicholi Vorsa⁵ · Juan Zalapa^{1,7}

Received: 16 March 2018 / Accepted: 19 June 2018 / Published online: 2 July 2018

© This is a U.S. Government work and not under copyright protection in the US; foreign copyright protection may apply 2018

Abstract

Because of its known phytochemical activity and benefits for human health, American cranberry (*Vaccinium macrocarpon* L.) production and commercialization around the world has gained importance in recent years. Flavonoid compounds as well as the balance of sugars and acids are key quality characteristics of fresh and processed cranberry products. In this study, we identified novel QTL that influence total anthocyanin content (TAcy), titratable acidity (TA), proanthocyanidin content (PAC), Brix, and mean fruit weight (MFW) in cranberry fruits. Using repeated measurements over the fruit ripening period, different QTLs were identified at specific time points that coincide with known chemical changes during fruit development and maturation. Some genetic regions appear to be regulating more than one trait. In addition, we demonstrate the utility of digital imaging as a reliable, inexpensive and high-throughput strategy for the quantification of anthocyanin content in cranberry fruits. Using this imaging approach, we identified a set of QTLs across three different breeding populations which collocated with anthocyanin QTL identified using wet-lab approaches. We demonstrate the use of a high-throughput, reliable and highly accessible imaging strategy for predicting anthocyanin content based on cranberry fruit color, which could have a large impact for both industry and cranberry research.

Keywords QTL mapping · Anthocyanin · Cranberry · High-throughput phenotyping · Imaging · Fruit phytochemicals

Communicated by S. Hohmann.

Electronic supplementary material The online version of this article (<https://doi.org/10.1007/s00438-018-1464-z>) contains supplementary material, which is available to authorized users.

✉ Luis Diaz-Garcia
diaz.antonio@inifap.gob.mx

✉ Juan Zalapa
jezalapa@wisc.edu; Juan.Zalapa@ars.usda.gov

- ¹ Department of Horticulture, University of Wisconsin, Madison, WI, USA
- ² Instituto Nacional de Investigaciones Forestales, Agrícolas y Pecuarias, Aguascalientes, Mexico
- ³ The Land Institute, Salina, KS, USA
- ⁴ Bayer CropScience NV, Innovation Center, Ghent, Belgium
- ⁵ Blueberry and Cranberry Research and Extension Center, Rutgers University, Chatsworth, NJ, USA
- ⁶ Valley Corporation, Tomah, WI, USA
- ⁷ USDA-ARS, Vegetable Crops Research Unit, University of Wisconsin, Madison, WI, USA

Introduction

The American cranberry (*Vaccinium macrocarpon* L.) is a diploid ($2n = 2x = 24$), woody perennial, temperate fruit crop well-adapted to the acidic bogs of North America (Pierre et al. 2013). Cranberry fruit is highly regarded because of the potential nutritional benefits of the flavonoids and other phytochemical compounds they contain (Ferguson et al. 2004; Bodet et al. 2008; Pappas and Schaich 2009; Shabrova et al. 2011). In the last decades, the cranberry industry has experienced a series of “boom and bust” cycles of economic expansion and contraction (Jesse et al. 1993). Traditionally, the goal of cranberry breeders in the United States has been to produce highly productive varieties, which together with the increment in acreage devoted to cranberry production, has resulted in an overproduction and low cranberry prices observed in recent years (McCown and Zeldin 2003; Vorsa and Johnson-Cicalese 2012). To fully exploit the current cranberry supply, fill niche markets (e.g., organic, fresh, and specialty products such as sweetened and dried fruit) and allow further industry expansion into health-oriented

products, it is vital for cranberry breeding programs to focus on novel cranberry characteristics and phytochemical constituents that provide value-added incentives to growers and processors.

Several studies have characterized the metabolic profile of cranberry fruits, specifically flavonoids, sugar conjugates, and acid composition, and established that the main anthocyanins present in cranberry are peonidin and cyanidin 3-galactosides, arabinosides, and glucoside anthocyanins (Vorsa and Polashock 2005). Additionally, it has been shown that cranberry fruits are rich in different types of proanthocyanidins (Foo and Porter 1980), which recently became object of extensive studies primarily because of their anti-bacterial, antiviral, and pharmacological activity in humans (Su et al. 2010; Feldman and Grenier 2012; Pierre et al. 2013), as well as for repelling herbivory and fungal pathogens (Dixon et al. 2005; Pappas and Schaich 2009). Accumulation of proanthocyanidins, anthocyanins, and other flavonoids have been studied through the ripening process in commercial cranberry cultivars and undomesticated materials (Wang et al. 2017). Vvedenskaya and Vorsa (2004) found that proanthocyanidin levels reached their maximum concentrations during flowering and early fruit set, and declined until fruit ripening, followed by slight increases during ripening. Conversely, anthocyanin glycosides increased over fruit development and maturation stages, with peonidin-3-galactoside and cyanidin-3-galactoside being the predominant compounds. Finally, it has been shown that cranberry fruit, like other berries, contain minor quantities of carotenes (Curl 1964).

Although studies regarding chemical composition are abundant, few genetic characterizations of the major chemical compounds key for cranberry industry have been carried out despite the recent availability of genetic and genomic resources. Georgi et al. (2013) published the first SSR-based genetic map of American cranberry, and reported several QTLs for yield, fruit weight, titratable acidity and proanthocyanidin content. With the recent development of high-density genetic maps (Schlautman et al. 2015, 2017; Covarrubias-Pazaran et al. 2016a; Daverdin et al. 2017), the creation of new mapping populations (Schlautman et al. 2015), the development of modern massive phenotyping techniques (Houle et al. 2010), and the availability of the cranberry genome (Polashock et al. 2014), the identification and fine-mapping of loci governing major phytochemicals in cranberry fruit are crucial for the future breeding of cultivars with enhanced phytochemical properties for processing and consumption.

In this study, we report a set of novel QTLs for important traits in cranberry fruits such as total anthocyanin content (TAcy), titratable acidity (TA), proanthocyanidin content (PAC), Brix, and mean fruit weight (MFW). Multiple breeding populations in this study enabled an extensive validation for incorporating linked molecular markers into cranberry

breeding strategies. Moreover, given the documented utility of imaging technologies for massive phenotyping and genetic association (Gonzalo and Van Der Knaap 2008; Xiao et al. 2009; Campbell et al. 2015), we demonstrate the use of a high-throughput, reliable and highly accessible imaging strategy for predicting anthocyanin content based on cranberry fruit color, which could have a large impact for both industry and cranberry research.

Methods

Plant material and experimental design

We performed quantification of total anthocyanin content (TAcy), proanthocyanidin content (PAC), titratable acidity (TA), Brix, and mean fruit weight (MFW) in a full-sib breeding population (CNJ02-01, $N=163$) over a 3-year period (2011–2014). This population was obtained by crossing the paternal parent CNJ97-105-4 ('Mullica Queen') and the maternal parent, NJS98-23 ('Crimson Queen'), and it is planted at Rutgers University P.E. Marucci Center, Chatsworth, NJ, USA. In addition during 2014, we digitally phenotyped a replicate of this population planted in Cranberry Creek Cranberries Inc., Necedah, WI, USA, as well as two more populations, CNJ04-02 ($N=64$, also planted at Cranberry Creek Cranberries Inc.) and GRYG ($N=267$, planted at Valley Corporation, Tomah, WI, USA). Because CNJ02-01 and CNJ04-02 share 'Mullica Queen' as a parent, these two populations represent half-sib families. The GRYG population was derived from a cross between the maternal parent [BGx(BLxNL)]95 and the paternal parent GH1 × 35.

All three populations (CNJ02-01, CNJ04-02, and GRYG) were established in a modified augmented design where check varieties were located in the borders of the plots. For the CNJ02-01 population, we obtained replicated measurements of chemical traits at two harvest season dates (September 15 and October 5) per year, for a 3-year period (2011–2013). Regarding digital phenotyping, we recorded data for all three populations only once during 2014.

Chemical analysis

All fruit chemistry traits were analyzed using standard industry methods described in Georgi et al. (2013). Specifically, PAC was measured spectrophotometrically using 4-dimethylaminocinnamaldehyde as a reagent at 640 nm (Wang et al. 2017); TAcy was measured spectrophotometrically under acidic conditions at 515 nm; Brix was measured as percent soluble solids using a refractometer; and TA (expressed as milliequivalents of citric acid) used 0.1 N NaOH and an endpoint of pH 8.1. Finally, MFW was determined by harvesting

all the cranberry fruits within a 0.09 m², and then, weighting a subsample of 100 fruits.

Imaging-based phenotyping

As described in Diaz-Garcia et al. (2016), TAcy in cranberry fruits can be predicted considerably well using digital imaging. Similar results have been found in sweet cherry (Taghadomi-Saberi et al. 2014), grape (Nogales-Bueno et al. 2015), and strawberry (Yoshioka et al. 2013). In this study, we took pictures of at least 25 fruits per genotype using a regular DSLR camera on a white background with controlled lighting conditions; for color normalization purposes, we included reference black circles on each picture. Then, we used GiNA (Diaz-Garcia et al. 2016) to automatically process all the images and extract color measurements per fruit. For each genotype, two different digital traits were computed; color intensity was calculated by averaging the pixel color values of each single fruit; similarly, color variation was the standard deviation of the pixel color values. Thus, at least 25 values were obtained per genotype for each digital trait.

Statistical analysis

For all populations (including chemical and digital phenotyping data), we fitted mixed models to estimate genomic Best Linear Unbiased Predictors (BLUPs) and calculate genomic heritabilities (h^2 , de los Campos et al. 2015). In particular, we used the function *mmer* of the R package *sommer* (Covarrubias-Pazaran 2016) following the author recommendations. For the chemical data, we treated each year/month combination separately, and once calculated the BLUP, we averaged the BLUP values among years for each of the months studied. Since a single repeated measurement was available for digital phenotyping traits, we fitted mixed models for each trait and BLUPs were directly used for QTL mapping. The mixed models used here had the form $Y = Zu + e$ was fitted, where Y represented the measured trait in a specific year (and month for the case of chemical traits), Z was the incidence matrices for random effects (identity matrix of length equals to the number of individuals), and u was a variance–covariance matrix (additive relationship matrix A). The kinship matrix A was constructed with the function *A.mat* from the *sommer* package, using only the bi-allelic markers. After this analysis, we ended up with two sets of BLUPs per chemical trait (for September and October, average of the 3-year period) for the CNJ02-01 population, and a single set per digital trait for all three populations (i.e., CNJ02-01, CNJ02-02, and GRYG); these datasets were used for QTL mapping (see below). All raw data and BLUPs are provided in Supplementary File 1.

QTL mapping

We performed QTL mapping using the function *scanone* (with the Haley-Knott regression method) from the R package *qtl* (Broman et al. 2003). The LOD score threshold to call significant QTL was calculated using a permutation test (1000 permutations) and a nominal significance level of 5%. We used a high-density composite map produced with 6073 markers spanning 12 linkage groups and a total length of 1130.42 cM (Schlautman et al. 2017); because of the high density of the markers used here, no additional marker imputation was needed. We identified significant peaks automatically using the function *big.peaks.col* from the package *Fragman* (Covarrubias-Pazaran et al. 2016b); QTLs separated from each other by more than 20 cM were considered different. We calculated 1.5 LOD-supporting intervals using a custom code. For each trait, the function *fitqtl* was used with all significant markers to quantifying the explained variance by QTL and the model.

Results

Phenotypic variation and genetic correlation between traits

For most of the chemical traits measured in the CNJ02-01 population, raw phenotypic measurements across genotypes were moderately consistent during the 3-year period as described below (Supplementary File 1). MFW presented the highest Pearson's correlation between years (mean $r=0.62$), whereas Brix had the lowest (mean $=0.16$), mainly because the low heritability observed in September of the first year of evaluation (Supplementary File 1). TAcy had a moderate correlation with a mean of 0.46, whereas TA and PAC had a mean correlation of 0.28 and 0.35, respectively. Due to zero or close-to-zero genetic variance, the data entries corresponding to Brix Sep 2013 and PAC Oct 2011 were not considered in further analysis. Mixed models considerably increased the correlation between years for all the traits (Fig. 1a, b). The most notable increments were observed for Brix and TA with increments greater than 200%. Mean year-to-year correlations were 0.66 for MFW, 0.68 for TAcy, 0.50 for Brix (Sep 2013 removed), 0.53 for TA, and 0.57 for PAC (Oct 2011 removed). Because of these results, we used the averages per month (from the 3-year period) in subsequent analyses.

Genetic correlations (between genomic BLUPs) were consistently higher when comparing the September and October measurements of the same trait (Fig. 1a). For example, the genetic correlation between September and October estimates were 0.86 for TA, 0.84 for MFW, 0.83 for TAcY and 0.6 for PAC; Brix had the lowest correlation (0.36)

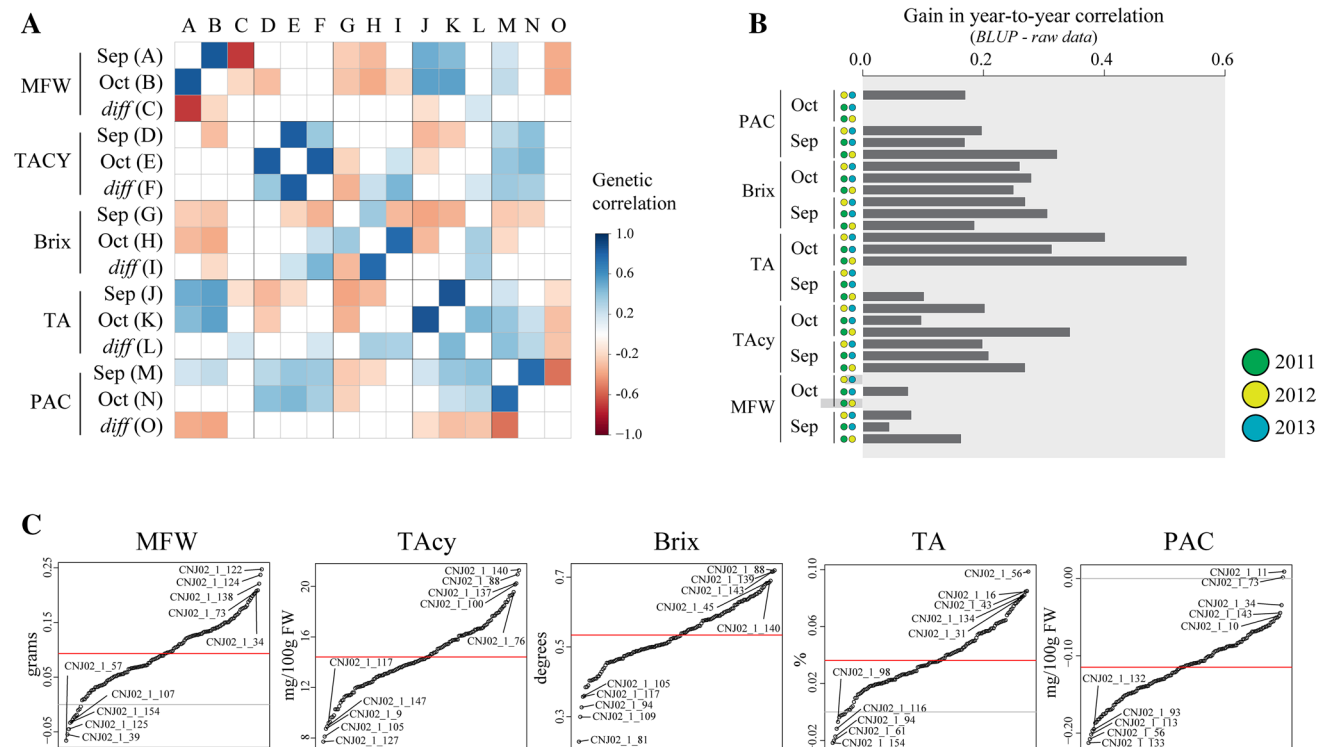


Fig. 1 Genetic correlation among traits and distribution of differential accumulation estimates (*diff*) for total anthocyanin content (TAcY), Brix, titratable acidity (TA), proanthocyanidin content (PAC) and mean fruit weight (MFW) evaluated in the CNJ02 population. **a** Genetic correlation between BLUPs (only significant correlations at

$p < 0.05$ are colored). **b** Gain in genetic correlation when comparing raw phenotypic values and BLUP estimates. **c** Differential accumulation measurements (*diff*) showing top and low performing materials (red and gray line indicates mean and zero, respectively). (Color figure online)

within months. Monthly repeated measurements were used to calculate the differential accumulation per trait during the evaluation period; henceforth, these traits are identified with the subscript *diff* (e.g., $TAcY_{diff} = \text{October } TAcY \text{ measurement} - \text{September } TAcY \text{ measurement}$; Fig. 1c). Differential accumulation measurements showed moderate to high correlation with their main traits. For example, MFW_{diff} had a correlation with MFW September and MFW October of -0.70 and -0.21 , respectively, whereas for TAcY, the correlation was 0.36 and 0.82 , respectively. Among the genetic correlations between traits, MFW and TA had the highest correlation coefficients (0.42 – 0.54), followed by TAcY and PAC (0.26 – 0.44).

Although the populations used in this study were created for breeding purposes (parental materials are advanced breeding selections or well-established cultivars), significant phenotypic variation was observed for all the traits evaluated (Table 1). For MFW, BLUPs ranged from 1.84 to 2.38 g (mean = 2.07 g) in September, and from 1.95 to 2.40 g (mean = 2.17 g) in October. For TAcY, large differences were observed between months with values ranging from 16.05 mg/100 g FW to 28.88 mg/100 g FW (mean = 22.35 mg/100 g FW) in September, and

from 26.32 mg/100 g FW to 48.90 mg/100 g FW (mean = 36.76 mg/100 g FW) in October. Brix showed little change with September values ranging from 8.42° to 8.72° (mean = 8.65°), whereas for October, values ranged from 8.86° to 9.34° (mean = 9.10°). Similarly, for TA values ranged from 2.37 to 2.58% (mean = 2.48%) in September, and from 2.38 to 2.61% (mean = 2.52%) in October. As expected, PAC showed a decrease over time with values ranging from 1.46 mg/100 g FW to 1.75 mg/100 g FW (mean = 1.61 mg/100 g FW) in September, and from 1.38 mg/100 g FW to 1.62 mg/100 g FW (mean = 1.50 mg/100 g FW) in October. In general, genomic heritabilities were low, from 0.12 (Brix, October) to 0.33 (MFW, September).

For most of the cultivars, the differential accumulation estimates were small; however, some accumulation values could be of interest for breeding purposes. For example, genotype CNJ02-01-140 possessed the largest $TAcY_{diff}$ (21.26 mg/100 g FW) as well as one of the top values in $Brix_{diff}$. Similarly, genotype CNJ02-01-122 had an increase in MFW of 0.25 g during the evaluation period. In Fig. 1c, differential accumulation measurements are shown for all the chemical traits evaluated in the CNJ02 population.

Table 1 Summary of BLUPs for mean fruit weight (MFW), total anthocyanin content (TAcy), Brix, titratable acidity (TA) and proanthocyanidin content (PAC) in the CNJ02-01 population

Trait ^a	Min	Max	Mean	Median	Q25 ^b	Q75 ^c	Top 5 genotypes	<i>h</i> ²
MFW Sep	1.84	2.38	2.07	2.07	1.99	2.16	CNJ02-01-38, CNJ02-01-57, CNJ02-01-25, CNJ02-01-39, CNJ02-01-23	0.33
MFW Oct	1.95	2.40	2.17	2.18	2.10	2.22	CNJ02-01-31, CNJ02-01-38, CNJ02-01-60, CNJ02-01-114, CNJ02-01-109	0.18
MFW _{diff}	-0.07	0.25	0.09	0.09	0.05	0.14	CNJ02-01-122, CNJ02-01-124, CNJ02-01-138, CNJ02-01-73, CNJ02-01-34	
TAcy Sep	16.05	28.88	22.35	21.99	20.33	24.43	CNJ02-01-126, CNJ02-01-67, CNJ02-01-88, CNJ02-01-63, CNJ02-01-148	0.36
TAcy Oct	26.32	48.90	36.76	36.46	33.41	40.06	CNJ02-01-88, CNJ02-01-140, CNJ02-01-76, CNJ02-01-2, CNJ02-01-100	0.52
TAcy _{diff}	7.71	21.26	14.41	14.21	12.45	16.31	CNJ02-01-140, CNJ02-01-88, CNJ02-01-137, CNJ02-01-100, CNJ02-01-76	
Brix Sep	8.42	8.72	8.56	8.56	8.52	8.60	CNJ02-01-30, CNJ02-01-154, CNJ02-01-75, CNJ02-01-151, CNJ02-01-155	0.15
Brix Oct	8.86	9.34	9.10	9.09	9.04	9.16	CNJ02-01-15, CNJ02-01-45, CNJ02-01-4, CNJ02-01-154, CNJ02-01-135	0.12
Brix _{diff}	0.23	0.72	0.53	0.53	0.48	0.60	CNJ02-01-88, CNJ02-01-139, CNJ02-01-143, CNJ02-01-45, CNJ02-01-140	
TA Sep	2.37	2.58	2.48	2.48	2.45	2.51	CNJ02-01-28, CNJ02-01-81, CNJ02-01-40, CNJ02-01-92, CNJ02-01-30	0.26
TA Oct	2.38	2.61	2.52	2.52	2.48	2.55	CNJ02-01-56, CNJ02-01-40, CNJ02-01-60, CNJ02-01-28, CNJ02-01-13	0.28
TA _{diff}	-0.02	0.10	0.04	0.03	0.02	0.06	CNJ02-01-56, CNJ02-01-16, CNJ02-01-43, CNJ02-01-134, CNJ02-01-31	
PAC Sep	1.46	1.75	1.61	1.61	1.56	1.66	CNJ02-01-82, CNJ02-01-137, CNJ02-01-28, CNJ02-01-25, CNJ02-01-156	0.24
PAC Oct	1.38	1.62	1.50	1.50	1.46	1.53	CNJ02-01-2, CNJ02-01-11, CNJ02-01-146, CNJ02-01-10, CNJ02-01-67	0.27
PAC _{diff}	-0.21	0.01	-0.11	-0.11	-0.14	-0.09	CNJ02-01-11, CNJ02-01-73, CNJ02-01-34, CNJ02-01-143, CNJ02-01-10	

^aUnits: MFW is grams, TAcy and PAC are in mg/100 g FW, Brix is in degrees, and TA is in percentage

^b25% quantile

^c75% quantile

Mapping of fruit chemical traits

For the CNJ02-01 population, we discovered over 80 significant associations across the genome for mean fruit weight, total anthocyanin content, titratable acidity, Brix, and proanthocyanin content (Fig. 2). From these, 20 were found in September, 33 in October, and 30 in the differential accumulation traits. MFW had the largest number of QTL with 20, followed by TA with 17, MFW and TAcy with 16 each, and Brix with 14. As expected, from these 80 QTLs we found multiple collocated QTLs for specific traits in the same positions when using the September, October, or differential accumulation measurements. A list with all the QTLs detected in this study, including location, marker name, LOD scores, as well as additional pertinent information, is provided in Table 2 and Supplementary File 1.

We identified a large QTL for MFW (average explained variance = 12.6%) in both September and October in LG3 position 32.9 cM. Additionally, we found more collocated QTLs in both months in chromosomes 1, 3 and 11, but with lower explained variances. Interestingly, only 2 out of 5 QTLs discovered for MFW_{diff} corresponded to QTL identified in either September or October; however, the remaining three explained only an average of 4.2% of the phenotypic

variation. In summary, QTL models for MFW in September, October, and MFW_{diff} explained 67.8, 70.8, and 51.1% of the phenotypic variation, respectively. A major QTL was discovered for TAcy in LG 3 position 56.18–58.6 cM, which explained the largest variation observed in this study (45.7% in September and 19.6% in October); surprisingly, this QTL was absent for TAcy_{diff}. TAcy October and TAcy_{diff} shared four QTLs (one in LG 1, two in LG 7, and one in LG 11). TAcy models including all discovered QTLs explained 58.4%, 78.7% and 66.5% of the total phenotypic variation of TAcy September, TAcy October, and TAcy_{diff}, respectively. For Brix, the largest QTL was identified in September at LG 7 position 52.2 cM (explained variance = 28.2%). Brix October and Brix_{diff} had three collocated QTLs in linkage groups 1, 3 and 12, from which the QTL in LG 1 explained up to 13.0% of the phenotypic variation. Brix_{diff} had the largest explained variance with 69.0%, followed by Brix October with 56.7%, and Brix September with only 41.2%. For TA there were no collocated QTL between TA_{diff}, TA September, or TA October; all 5 QTLs detected for TA_{diff} corresponded to unique positions. When comparing TA September and TA October, three collocated QTLs were found in LG 11 position 53 cM, LG 4 position 11 cM–18 cM, and LG 5 position 47 cM. QTL models for TA explained 57.7,

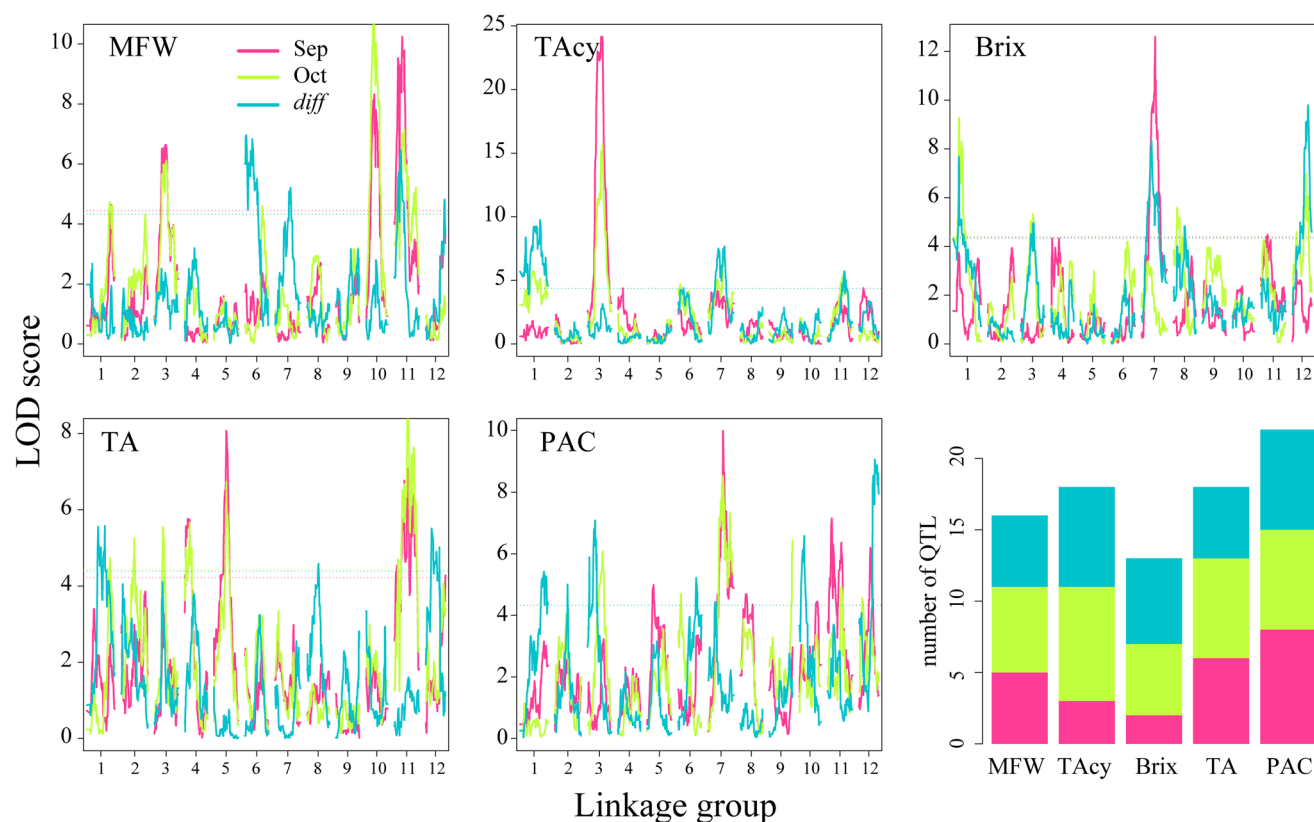


Fig. 2 LOD score profiles for mean fruit weight (MFW), total anthocyanin content (TAcY), Brix, titratable acidity (TA) and proanthocyanidin content (PAC), in the CNJ02-01 population. As indicated in the first panel legend, pink, red and blue lines indicate September, October and differential accumulation (*diff*) profiles, respectively. Using

72.0 and 41.1% for TA September, TA October and TA_{diff}, respectively. Out of the eight QTLs found for PAC September, two were collocated with QTL for PAC October at linkage groups 7 and 11, of which the first one explained, in average, 9.0% of the phenotypic variance. PAC_{diff} had not collocated QTL with neither PAC Sep or PAC Oct. QTL models explained 64.2% for PAC September, 67.4% for PAC October, and 71.7% for PAC_{diff}.

Digital-based anthocyanin quantification

We performed digital phenotyping in the CNJ02-01, CNJ04-02 and GRYG populations to estimate color intensity and color variation in cranberry fruits. Although we recorded all three RGB channels for each fruit, we used only the red channel because it showed the highest correlation with TAcY content (−0.78 for TAcY September and −0.85 for TAcY October; digital color scales are inverted, that is why the negative correlation). Genomic heritabilities for color intensity and color variation ranged from 0.50 to 0.79 for all three populations, except for the GRYG population which had 0.23 for color variation. The genetic correlation between

similar colors, significant thresholds ($p=0.05$, based on 1000 permutations) are indicated as horizontal lines. In the last panel, a summary showing QTL counts by month and trait is provided. A complete list of QTL can be found in Supplementary File 1. (Color figure online)

color intensity and color variation was greater than 0.98 for both CNJ02-01 and CNJ04-02 populations, and 0.67 for the GRYG population. These variation may be explained by fact that the GRYG population had more uniformly colored fruits than the other two populations. As a note, we harvested the GRYG population 2 weeks after the CNJ02-01 and CNJ04-02, which allowed time to genotypes with uncolored fruit to fully color. In general terms, the high correlation between color intensity and color variation indicates that lighter colored fruits tend to be highly variable in color.

As described before, we phenotyped the CNJ02-01 population for both chemical and digital traits; however, different plantings were used on each approach. Despite that, the genetic correlation between color intensity and TAcY for this population was −0.78 and −0.85 for September and October, respectively (these correlation estimates correspond to the ones provided above).

QTL mapping of digital traits

Using digital phenotyping data, we compared the number and position of QTLs identified through TAcY

Table 2 QTL for the chemical traits mean fruit weight (MFW), total anthocyanin content (TAcy), Brix, titratable acidity (TA), and proanthocyanidin content (PAC), and the digital traits color intensity and color variation, discovered in all three populations

Trait	LG	Position (cM)	Nearest marker	LOD score	1.5 LOD support interval	R^2 (by QTL)	R^2 (by the model)	Population
<i>Chemical traits</i>								
TAcy Sep	3	56.2	scf5304	23.0	10.3	39.5	62.3	CNJ02
	4	18.5	scaffold_60960_209	3.2	22.9	3.9	62.3	
	12	19.3	scaffold_27631_2392	3.7	26.1	4.6	62.3	
TAcy Oct	1	62.8	X1trimcontig440230	2.2	30.0	1.5	78.7	
	1	85.2	scaffold_5299_7068	0.3	44.8	0.2	78.7	
	1	106.9	scaffold_12748_4113	1.9	16.3	1.3	78.7	
	3	58.6	SCF85773	21.0	10.3	19.6	78.7	
	6	7.9	scaffold_430_12130	5.3	15.9	3.8	78.7	
	7	35.7	scaffold_30468_976	4.1	45.8	2.9	78.7	
	7	62.0	SCF128015	4.0	12.9	2.8	78.7	
	11	64.5	scaffold_2406_6866	8.0	7.2	6.0	78.7	
TAcy diff	1	52.1	scaffold_18380	1.1	18.8	2.1	41.1	
	1	77.9	scaffold_41901_298	3.0	15.9	5.7	41.1	
	8	43.5	SCF71184	2.7	24.8	5.1	41.1	
	12	25.1	scaffold_49589_2014	1.6	34.1	3.0	41.1	
	12	55.0	SCF38942	1.4	37.4	2.6	41.1	
TA Sep	4	11.3	scaffold_42755_943	7.3	23.5	9.3	63.8	
	5	47.1	scaffold_218000_24	6.0	9.5	7.5	63.8	
	11	9.6	scaffold_125_21038	6.0	17.8	7.4	63.8	
	11	53.0	SCF120937	2.6	8.4	3.1	63.8	
	11	75.6	scaffold_28041_700	2.9	16.7	3.4	63.8	
	12	77.6	scaffold_84992	5.0	13.2	6.1	63.8	
TA Oct	1	98.0	scaffold_1825_2736	5.5	17.5	5.2	71.9	
	2	49.4	scaffold_77675_473	7.4	10.3	7.3	71.9	
	3	33.4	X82171_K70	7.2	10.6	7.0	71.9	
	4	18.6	scaffold_27846_3448	1.7	16.5	1.5	71.9	
	5	47.7	scaffold_55702_1668	11.8	11.4	12.5	71.9	
	11	31.2	scaffold_62302_445	2.3	56.2	2.1	71.9	
	11	53.0	SCF120937	2.6	9.0	2.3	71.9	
	12	55.0	SCF38942	1.4	37.4	2.6	41.1	
TA diff	1	52.1	scaffold_18380	1.1	18.8	2.1	41.1	
	1	77.9	scaffold_41901_298	3.0	15.9	5.7	41.1	
	8	43.5	SCF71184	2.7	24.8	5.1	41.1	
	12	25.1	scaffold_49589_2014	1.6	34.1	3.0	41.1	
	12	55.0	SCF38942	1.4	37.4	2.6	41.1	
Brix Sep	7	52.2	scaffold_16505_2290	12.6	3.0	28.2	41.2	
	11	26.1	Pr031818821_185	4.5	37.0	8.8	41.2	
Brix Oct	1	31.7	scaffold_50850_1690	8.4	2.6	13.0	56.7	
	3	47.0	scaffold_20817_2608	5.3	20.8	7.8	56.7	
	8	14.7	SCF107477	6.7	13.2	10.1	56.7	
	12	19.3	scaffold_4159_1157	1.5	25.9	2.0	56.7	
	12	55.0	scaffold_43277_235	1.6	7.1	2.1	56.7	
Brix diff	1	30.6	scaffold_44200_416	8.2	2.6	9.0	68.9	
	3	50.6	scaffold_46587_1839	8.0	23.2	8.8	68.9	
	7	38.3	scaffold_164771_190	3.2	12.3	3.3	68.9	
	7	60.6	scaffold_20427_5005	3.2	46.1	3.3	68.9	
	8	42.8	scaffold_51524_72	6.7	13.1	7.2	68.9	
	12	63.1	scaffold_147305_234	5.0	12.9	5.2	68.9	

Table 2 (continued)

Trait	LG	Position (cM)	Nearest marker	LOD score	1.5 LOD support interval	R^2 (by QTL)	R^2 (by the model)	Population
PAC Sep	5	24.3	scaffold_143782_351	5.0	28.9	5.1	70.1	
	7	56.1	scaffold_30770_2900	9.0	7.5	9.7	70.1	
	8	22.3	scaffold_52659_1515	1.4	42.8	1.3	70.1	
	8	47.0	scaffold_40880_1057	1.7	45.2	1.6	70.1	
	10	70.8	scaffold_7286_3907	4.1	17.9	4.1	70.1	
	11	16.4	scaffold_170652_55	5.3	9.1	5.4	70.1	
	11	53.0	scaffold_51138_759	2.1	16.7	2.0	70.1	
	12	46.3	scaffold_6406_7899	5.5	11.2	5.6	70.1	
PAC Oct	3	58.6	SCF85773	3.8	23.5	4.1	67.4	
	6	11.1	GVC.V31e03_240	2.6	17.9	2.7	67.4	
	7	56.1	scaffold_15867_4759	7.4	8.4	8.4	67.4	
	7	82.6	scaffold_43434_633	1.8	5.7	1.8	67.4	
	9	89.9	contig259Fb	7.8	2.9	9.0	67.4	
	11	53.0	SCF120937	3.3	10.7	3.5	67.4	
PAC diff	12	14.6	scaffold_58926_848	5.3	26.7	5.8	67.4	
	1	100.4	scaffold_81716_1234	2.9	30.3	2.7	71.7	
	2	49.4	scaffold_77675_473	4.0	9.1	3.8	71.7	
	3	30.2	scaffold_57070_1345	7.2	14.0	7.1	71.7	
	6	69.2	scaffold_24568_3388	5.7	18.3	5.5	71.7	
	7	28.6	scaffold_20940_1397	2.9	10.8	2.7	71.7	
MFW Sep	10	20.9	scaffold_6013_884	6.8	23.4	6.6	71.7	
	12	63.1	scaffold_147305_234	10.6	22.6	11.0	71.7	
	1	103.2	scaffold_19539_410	3.2	9.7	3.3	67.8	
	3	45.5	scaffold_12440_4793	11.7	26.4	14.1	67.8	
	10	32.9	scaffold_12381_1637	8.5	15.7	9.7	67.8	
	11	30.3	scaffold_28856_2095	12.8	9.7	15.8	67.8	
MFW Oct	12	74.9	scaffold_34492_1275	3.8	9.8	4.1	67.8	
	1	95.4	scaffold_185_4067	4.6	19.9	4.5	70.8	
	3	47.0	scaffold_20817_2608	9.6	24.3	10.2	70.8	
	6	66.8	scaffold_97576_996	6.1	17.0	6.1	70.8	
	10	32.9	scaffold_12381_1637	13.7	14.4	15.5	70.8	
	11	38.1	scaffold_40899_1890	6.9	22.5	7.0	70.8	
MFW diff	11	82.5	scaffold_56714_991	3.4	21.3	3.3	70.8	
	6	5.2	scaffold_15239_3508	2.2	11.1	3.5	51.1	
	6	28.2	scaffold_57397_425	1.6	25.6	2.5	51.1	
	7	59.0	X1trimcontig337780	4.1	21.3	6.7	51.1	
	11	24.5	scaffold_113473_310	3.9	11.1	6.4	51.1	
	12	74.9	scaffold_34492_1275	4.9	6.8	8.1	51.1	
<i>Digital phenotyping</i>								
Color intensity	3	8.8	scaffold_69755_831	19.2	3.1	16.1	59.0	GRYG
	3	33.4	scaffold_70042_968	20.2	12.3	17.1	59.0	GRYG
	3	36.5	scaffold_3243_9538	4.7	3.6	4.7	68.2	CNJ02
	3	54.2	scaffold_52119_1893	10.1	4.0	37.3	65.1	CNJ04
	3	58.6	SCF85773	6.2	8.8	6.4	68.2	CNJ02
	4	2.4	scf105g	1.8	2.1	4.7	65.1	CNJ04
	4	18.5	X5ms2b12	2.3	7.9	2.2	68.2	CNJ02
	6	7.9	scaffold_430_12130	3.0	13.3	3.0	68.2	CNJ02
	6	20.6	scaffold_6018_7390	7.2	13.5	5.4	59.0	GRYG
	6	40.5	scaffold_38187_2604	6.3	5.7	6.5	68.2	CNJ02
	11	50.1	scaffold_7078_6962	11.3	14.0	12.5	68.2	CNJ02

Table 2 (continued)

Trait	LG	Position (cM)	Nearest marker	LOD score	1.5 LOD support interval	R^2 (by QTL)	R^2 (by the model)	Population
Color variation	1	30.3	scaffold_6151_1214	6.6	6.0	4.7	60.8	GRYG
	3	33.4	scaffold_13562_2793	22.9	2.6	19.0	60.8	GRYG
	3	36.5	scaffold_3243_9538	3.5	14.7	3.4	69.0	CNJ02
	3	54.2	scaffold_52119_1893	10.4	4.0	37.7	66.1	CNJ04
	3	58.6	SCF85773	8.2	5.2	8.4	69.0	CNJ02
	4	2.4	scaffold_9495_6618	2.2	2.1	6.0	66.1	CNJ04
	4	18.5	X5ms2b12	1.9	7.9	1.8	69.0	CNJ02
	6	7.9	scaffold_430_12130	2.9	13.3	2.8	69.0	CNJ02
	6	40.5	scaffold_38187_2604	6.1	5.7	6.1	69.0	CNJ02
	9	68.1	scaffold_11828_430	2.9	11.5	2.0	60.8	GRYG
	9	88.5	scaffold_1155_331	0.5	18.7	0.3	60.8	GRYG
	10	47.2	scaffold_39489_1268	10.7	9.7	7.9	60.8	GRYG
	11	43.1	scaffold_49289_770	13.2	13.8	14.7	69.0	CNJ02
	12	12.2	scaffold_803_11742	1.8	6.2	1.3	60.8	GRYG
	12	41.7	scaffold_1179_7946	3.8	6.1	2.6	60.8	GRYG

quantification versus digital phenotyping. When digital phenotyping traits were used, we discovered 26 QTLs across all three populations, and from these, 10 corresponded to color intensity and 16 to color variation. The CNJ02-01 population had the largest number of QTLs with 12, followed by GRYG with 10 and CNJ04-02 with only 4. We expected to detect novel QTL, have better resolution, and higher QTL power detection because the increased precision of the image-based phenotyping approach employed here. Thus, the two QTLs found through TAcY quantification in LG 4 position 18.45 cM and LG 6 position 7.85 cM were located using digital traits in the CNJ02-01 population (the first one located in the same marker bin, the second one matched the exact genetic marker). More importantly, the largest QTL discovered in LG 3 position 56.18–58.58 cM, discovered for September and October data, was found in both of the CNJ02-01 and CNJ04-02 populations. Additionally, we identified a large QTL in the CNJ02-01 and GRYG populations around positions 33.36–36.59 cM of the same linkage group, which supports the presence of two QTLs in linkage group 3. For this particular case, we tested the presence of two closely located QTLs in LG 3 using the *scantwo* function of the R/ *qtl* package (Broman et al. 2003). This procedure is useful when dealing with closely located QTL, especially when their effects are of opposite directions, since it performs a two-dimensional, two-QTL scan through maximum likelihood. For color intensity in all three populations (Fig. 3a, upper panels), we found evidence that supports the presence of at least two additive QTL in linkage group 3; the first QTL corresponded to the region previously identified (55–58 cM), whereas the location of the second one varied across populations (in the range 10–38 cM). In contrast,

scantwo analysis on TAcY showed more consistency since QTL were found at positions 35 cM and 55–58 cM using September, October and differential accumulation data. For both cases (TAcY and digital color intensity), evidence of interacting QTL in linkage group 3 was weak (upper-left triangles, all with LOD score < 6).

To visually compare the effect of QTL in LG group 3 position 58 cM, we plotted the digital representations of the fruit colors observed in the pictures, classifying them by their corresponding genotypes. The marker at this position was of the form AB × CD, with the possible outcomes AC, AD, BC and BD. As previously mentioned, the color intensity trait used herein was derived from the red channel measurements, which had the highest correlation with TAcY. Because RGB values for single-fruit level were available, we colored each circle with the color observed in the original pictures (Fig. 3b). As observed, it is clear that both AC and AD genotypes had a larger amount of yellow fruit; conversely, BC and BD had larger amounts of darker fruits. To further understand these results, we compared density plots per genotype across all RGB channels. As expected, AC and AD genotypes had a shift in mean value in both red and green channels.

Finally, based on digital phenotyping, we found more QTLs in other linkage groups for all three populations; however, these showed low consistency in terms of collocation across populations, and in general, explained a minimal phenotypic variance. Additionally, because of the high genetic correlation between color intensity and color variation, most of the QTLs found for these two traits were likely redundant; we believe that both traits are measuring the same fruit characteristic. For further details, a complete list of QTLs

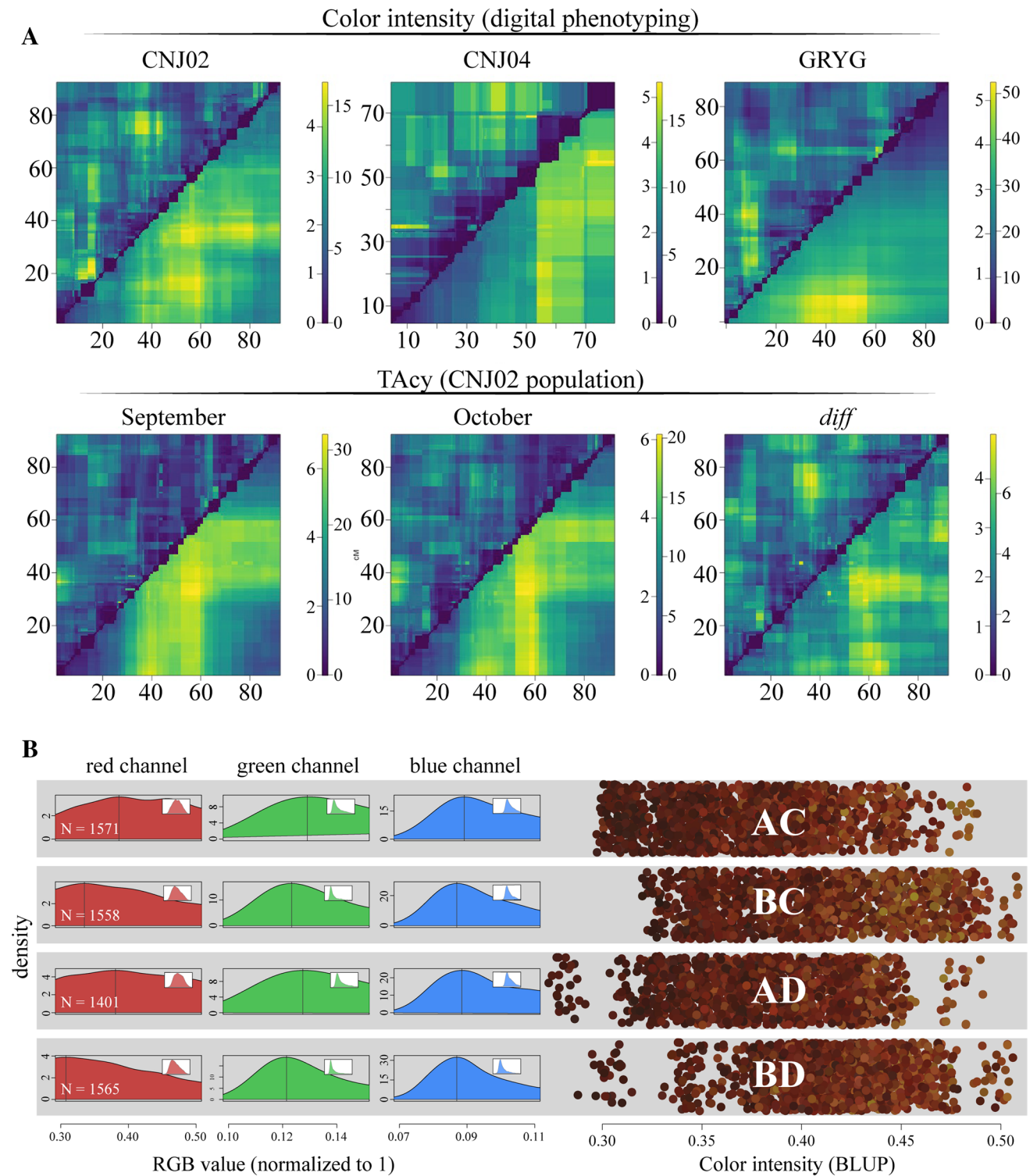


Fig. 3 a *Scantwo* plots of linkage group 3 for color intensity and total anthocyanin accumulation (TAcy) in the CNJ02-01, CNJ04-02 and GRYG populations. Lower-right and upper-left triangles show additive (*fv1*) and interaction models, respectively; units in both *x* and *y* axes are in cM; color bars on each *scantwo* plot display LOD scores for additive (in the left) and interaction (in the right) models. **b** Effect plot (by marker genotype) of QTL at linkage group 3 position 58 cM. On the right, circles correspond to single fruits of all evaluated genotypes. Circle locations in the *x* axis correspond to the

BLUP (derived from the red channel) used for QTL mapping, but it is colored according with the original RGB values from the photo; jittering was applied in the *y* axis to maximize visual comparison. On the left, pixel density plots per channel and genotype are displayed. Small windows inside each plot show the complete density distribution, and main plots, show zoomed version in the maximum values (black vertical line); *N* values correspond to the amount of fruits per genotypic category. (Color figure online)

discovered through digital phenotyping is provided in Supplementary File 1.

Color-linked marker segregation in yellow/red population

Several studies have described both major genes, that turn on and off anthocyanin biosynthesis accumulation, and minor genes responsible for accumulating different types and amounts of specific anthocyanins (Honda et al. 2002; Jaakola 2002). To investigate if any of the anthocyanin QTLs discovered in this study are acting as the on/off switch in the production of pigment, we analyzed the co-segregation of SSR markers within a diverse collection of commercial cultivars (that produce red mature fruit) and germplasm that produce yellow fruit only (derived from a yellow non-accumulating mutant called ‘Yellow Bell’). Using the SSR marker data published by Schlautman et al. (2015), we selected 12 SSR markers near to the QTL in linkage group 3, in particular, those in regions ~30, ~55 and ~80 cM; additionally, we included SSR in other LG that had minor QTL such as the ones in LG 6, LG 7, LG 10 and LG 11. Using these markers, we evaluated 96 cranberry accessions (48 red and 48 yellow fruiting accessions) and performed a Cramer’s *V* test using the R package *cramer*. The most significant associations (i.e., markers that co-segregated with color) corresponded to the markers in the range 55–60 cM of linkage group 3; markers in position ~30 and ~80 cM showed no clear co-segregation (Fig. 4).

Discussion

With over 150 different chemical compounds, cranberry fruit is a highly rich source of phytochemicals (Pappas and Schaich 2009). The function that these constituents (sugars, phenolics, proanthocyanidins, flavonols, anthocyanins, etc.) provide in plants is very diverse, including the attraction of beneficial insects, UV protection, pathogen defense, energy storage, and structural (Bulgakov et al. 2017). Similarly, these compounds are highly beneficial for human health because of their activity as antioxidants, anti-bacterial, anti-inflammatory, and anti-adhesion towards viral pathogens (Marwan and Nagel 1986; Gupta et al. 2007; Liu et al. 2011; Shabrova et al. 2011; Feldman and Grenier 2012). Given the importance of these compounds for cranberry industry, the set of QTLs discovered in this study represents an important resource that can be incorporated into different strategies for cranberry molecular breeding programs.

CN02-01 and CN04-02 represent 3rd and 4th breeding and selection cycle populations where yield, fruit size and color development were principal selection criteria. Thus, some allelic fixation for loci impacting these traits may have

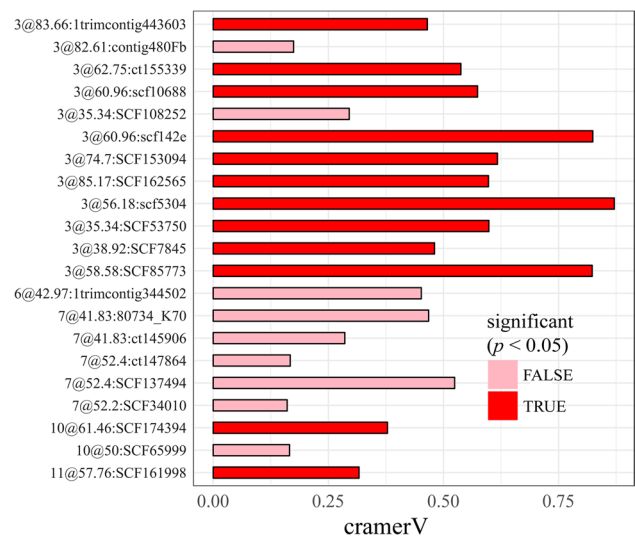


Fig. 4 Strength of association between SSR markers at major anthocyanin QTL positions, and fruit color (yellow/red). For each selected SSR, significance according with Cramer’s *V* test is displayed. (Color figure online)

occurred. However, we observed a large phenotypic variation for fruit weight and anthocyanin content, which are crucial when determining crop sale price in the cranberry industry. The CNJ02-01 population used in this study (as well as the CNJ04-02 and GRYG populations) were created for breeding purposes and not for genetic mapping; therefore, some of the materials evaluated here can be selected at any time and used in further breeding generations. According with the industry standards in the US, TAcy must be at least 30 mg/100 FW to obtain the best revenue for growers; thus, some of the accessions evaluated here could have great potential for commercial purposes (30 materials with TAcy October > 40 mg/100 FW). Additionally, a large proportion of materials (i.e., CNJ02-01-140, CNJ02-01-88, CNJ02-01-137, CNJ02-01-100 among others), showed not only high TAcy values, but a rapid increase in anthocyanin accumulation (> 20 mg/100 FW) from September to October. Moreover, materials such as CNJ02-01-140 and CNJ02-01-88 showed a large increase in Brix, which makes them ideal candidates to use during breeding. Besides, fruit weight and anthocyanin content, proanthocyanidins have gained importance due to their benefits for human health, and as discussed before, multiple accessions presented medium to high values for both TAcy and PAC (i.e., CNJ02-01-137, CNJ02-01-76), which makes multi-trait selection easier. As far as we know, there has not been any formal studies regarding how Brix and acidity levels in cranberry fruits impact sensory properties. In other fruit crops (Harker et al. 2002; Jayasena and Cameron 2008), it has been shown that Brix/acid ratio can be a very objective measurement that reflects the consumer acceptability for a fruit product (compared with the

use both chemicals independently), as well as an excellent indicator to determine the optimum harvesting period. Here, a rapid calculation of Brix/acidity ratio showed a distribution that does not correlate with the rest of the chemical traits measured (Supplementary File 1), but that highlights some materials with consistent high values for both September and October (i.e. CNJ02-01-154, CNJ02-01-97, CNJ02-0136). Without a doubt, the balance between sweetness and acidity is a primary aspect that dictates the quality of fruits, especially in cranberry, which has a short domestication history and limited genetic improvement for most traits.

The overall dynamics in chemical composition across time observed in this study was consistent with previous studies. Vorsa and Polashock (2000) found that harvest date affects significantly the total anthocyanin content, total phenolics and proanthocyanidins. Specifically, TAcY tends to increase over time whereas phenolics and proanthocyanidins decrease (Vvedenskaya and Vorsa 2004). Here, anthocyanin content increased from 22.4 mg/100 FW to 36.8 mg/100 FW, and proanthocyanidin content decreased from 1.6 mg/100 FW to 1.5 mg/100 FW. Moreover, the heritability estimates obtained here are consistent with previously reported studies, such as Vorsa and Johnson-Cicalese (2012), who used midparent-progeny mean regression, and found medium to high heritabilities for fruit weight (0.73–0.92) and TAcY (0.61–0.80), while Brix and titratable acidity showed highly variable and low heritabilities (<0.51).

Our study measured TAcY, Brix, TA, and PAC at two different harvest dates. As in many other fruit crops, cranberry phytochemical level testing is a requirement during the several weeks or months that takes to harvest the crop. Moreover, appropriate or exceeding levels in certain chemical quality tests can provide an economic incentive and increased revenue for growers. In the last decades, several studies have focused in understanding the different physiological mechanisms that affect cranberry fruit set (Birrenkott and Stang 1990; Roper et al. 1992, 1993), flower development (Lacroix 1926; Kaczmarska 2009), dormancy (Eady and Eaton 1972), seasonal chemical composition (Hagidimitriou and Roper 1994; Vvedenskaya and Vorsa 2004), and environment interaction and physiological response (Forsyth and Hall 1967; Eaton and Mahrt 1977; Vanden Heuvel and Davenport 2005). Using these background information, current cranberry programs are specifically developing high yielding, early and late cultivars with desirable levels of key chemicals such as anthocyanins, acids, and sugars. (McCown and Zeldin 2003; Wang et al. 2017). For the key traits evaluated in this study, we observed that the correlation between September and October BLUPs was generally high except for Brix. For further studies, we propose to separate the time between harvests, or adding further harvest dates to better understand seasonal changes in fruit chemistry composition.

Under the assumption that more closely related genotypes have similar phenotypes, we applied mixed models using genetic relationship information to obtain more precise breeding values (and a higher year-to-year genetic correlation). Nowadays, the studies regarding QTL mapping for quality traits in cranberry are limited. The first study was carried out by Georgi et al. (2013), in which multiple QTLs for fruit weight and titratable acidity were discovered; however, the very low marker density used to construct the genetic map limits the comparison with the QTL localized here. Later, Schlautman et al. (2015) generated a denser SSR-based genetic map and performed QTL mapping for fruit weight and other yield-related traits; interestingly, we found several collocated QTLs, particularly, those in LG 11.

In this study, we detected a large number of QTLs in chromosome 3 for total anthocyanin content and digital color traits. Observations based on the two-dimensional, two-QTL genome scan, show a complex mechanism that determines anthocyanin accumulation in cranberry, and requires further investigation. Additionally, the co-localization of a QTL for both anthocyanin and proanthocyanin content (LG 3, position 59 cM) is expected given that these two compounds are produced within the same biochemical pathway, and are dependent on each other. Mapping studies comparing the location of anthocyanin and proanthocyanidin-related QTL are limited; however, a recent study in red rice found at least two collocated QTLs for anthocyanin content and proanthocyanins (Xu et al. 2017). Using the locations of QTL for anthocyanin content, we attempted to identify candidate genes; however, our search was limited by the highly fragmented cranberry genome available. Proposing a regulation model to explain anthocyanin biosynthesis based solely in the QTL data presented here is premature. However, our analysis with SSR evaluated in a set of red/yellow unrelated cranberry accessions provided evidence of a major gene (at 55–60 cM of linkage group 3) possibly acting as a genetic switch to turn on or off pigmentation accumulation in cranberry.

Measuring chemicals using wet-lab methods is time-consuming and potentially error prone. For example, TAcY is estimated by averaging the anthocyanin content of a few fruits (i.e., 500 g) processed as a single sample, where information regarding the uniformity in anthocyanin content deposition around each individual fruit is lost. Using image-based phenotyping, data can be recorded at fruit level, thus providing not only information about the total color of each fruit, but also the uniformity of the pigment accumulation. In the cranberry industry, knowing uniformity in fruit anthocyanin content is very useful when determining the processing wanted to be achieved. On the other hand, with image analysis becoming more accessible for plant breeders, a more extensive characterization of plant phenotypes and their interaction with the environment can be achieved.

Acknowledgements This project was supported by USDA-SRCI Grant 2008-51180-04878; USDA-NIFA-AFRI 2013-67013-21107; USDA-ARS (Project Nos. 3655-21220-001-00 and 5090-21220-003-00 provided to J.Z.); WI-DATCP (SCBG Project #14–002); Ocean Spray Cranberries, Inc.; Wisconsin Cranberry Growers Association; NJ Cranberry and Blueberry Research Council; Cranberry Institute. LDG and GCP were supported by the Consejo Nacional de Ciencia y Tecnología (Mexico). LDG was also supported by the UW-Madison Gabelman-Seminis Distinguished Graduate Research Fellowship. BS was supported by the UW-Madison Frank B. Koller Cranberry Fellowship Fund for Graduate Students. AM was supported by the UW-Madison Biotechnology Training Program (BTP), National Institutes of Health training Grant (NIH 5 T32 GM08349; <http://www.nih.gov/>). We thank Eric Weisman for all his help in the lab, and also thank Cranberry Creek Cranberries Inc., Necedah, WI, USA for their collaboration and support during this project. J.Z. and B.S. wish to express their gratitude through 1 Cor 10:31. We thank the anonymous reviewers who helped enhance the quality of this paper.

Author contributions Designed the research: LDG, NV, JJC, JZ and BS. Contributed the mapping populations and performed part of the phenotyping: NV, JJC, and EG. Performed the experiment: LDG, BS and GCP. Analyzed the data: LDG and AM. Wrote the manuscript: LDG, BS and JZ. All coauthors reviewed and approved the final version of this manuscript.

Compliance with ethical standards

Conflict of interest The authors declared they had no conflict of interest.

Ethical approval The experiments in this manuscript compiled with the current laws of the country in which they were performed.

References

- Birrenkott B, Stang E (1990) Selective flower removal increases cranberry fruit set. *HortScience* 25:1226–1228
- Bodet C, Grenier D, Chandad F et al (2008) Potential oral health benefits of cranberry. *Crit Rev Food Sci Nutr* 48:672–680
- Broman KW, Wu H, Sen S, Churchill GA (2003) R/qtl: QTL mapping in experimental crosses. *Bioinformatics* 19:889–890. <https://doi.org/10.1093/bioinformatics/btg112>
- Bulgakov VP, Avramenko TV, Tsitsiashvili GS (2017) Critical analysis of protein signaling networks involved in the regulation of plant secondary metabolism: focus on anthocyanins. *Crit Rev Biotechnol* 37:685–700
- Campbell MT, Knecht AC, Berger B et al (2015) Integrating image-based phenomics and association analysis to dissect the genetic architecture of temporal salinity responses in rice. *Plant Physiol* 168:1476–1489. <https://doi.org/10.1104/pp.15.00450>
- Covarrubias-Pazarán G (2016) Genome-Assisted prediction of quantitative traits using the r package sommer. *PLoS One*. <https://doi.org/10.1371/journal.pone.0156744>
- Covarrubias-Pazarán G, Diaz-García L, Schlautman B et al (2016a) Exploiting genotyping by sequencing to characterize the genomic structure of the American cranberry through high-density linkage mapping. *BMC Genom*. <https://doi.org/10.1186/s12864-016-2802-3>
- Covarrubias-Pazarán G, Diaz-García L, Schlautman B et al (2016b) Fragman: an R package for fragment analysis. *BMC Genet*. <https://doi.org/10.1186/s12863-016-0365-6>
- Curl AL (1964) The carotenoids of several low-carotenoid fruits. *J Food Sci* 29:241–245. <https://doi.org/10.1111/j.1365-2621.1964.tb01725.x>
- Daverdin G, Johnson-Cicalese J, Zalapa J et al (2017) Identification and mapping of fruit rot resistance QTL in American cranberry using GBS. *Mol Breed*. <https://doi.org/10.1007/s11032-017-0639-3>
- de los Campos G, Sorensen D, Gianola D (2015) Genomic Heritability: What Is It? *PLoS Genet*. <https://doi.org/10.1371/journal.pgen.1005048>
- Diaz-García L, Covarrubias-Pazarán G, Schlautman B, Zalapa J (2016) GiNA, an Efficient and high-throughput software for horticultural phenotyping. *PLoS One*. <https://doi.org/10.1371/journal.pone.0160439>
- Dixon RA, Xie DY, Sharma SB (2005) Proanthocyanidins—a final frontier in flavonoid research? *New Phytol* 165:9–28
- Eady F, Eaton G (1972) Effects of chilling during dormancy on development of the terminal bud of the cranberry. *Can J Plant Sci* 279:273–279. <https://doi.org/10.4141/cjps72-044>
- Eaton GW, Mahrt BJ (1977) Cold hardiness testing of cranberry flower buds. *Can J Plant Sci* 57:461–465. <https://doi.org/10.4141/cjps77-067>
- Feldman M, Grenier D (2012) Cranberry proanthocyanidins act in synergy with licochalcone A to reduce *Porphyromonas gingivalis* growth and virulence properties, and to suppress cytokine secretion by macrophages. *J Appl Microbiol* 113:438–447. <https://doi.org/10.1111/j.1365-2672.2012.05329.x>
- Ferguson PJ, Kurowska E, Freeman DJ et al (2004) A flavonoid fraction from cranberry extract inhibits proliferation of human tumor cell lines. *J Nutr* 134:1529–1535
- Foo LY, Porter LJ (1980) The phytochemistry of proanthocyanidin polymers. *Phytochemistry* 19:1747–1754. [https://doi.org/10.1016/S0031-9422\(00\)83807-8](https://doi.org/10.1016/S0031-9422(00)83807-8)
- Forsyth F, Hall I (1967) Rates of photosynthesis and respiration in leaves of the cranberry with emphasis on rates at low temperatures. *Can J Plant Sci* 47:19–23
- Georgi L, Johnson-Cicalese J, Honig J et al (2013) The first genetic map of the American cranberry: Exploration of synteny conservation and quantitative trait loci. *Theor Appl Genet* 126:673–692. <https://doi.org/10.1007/s00122-012-2010-8>
- Gonzalo MJ, Van Der Knaap E (2008) A comparative analysis into the genetic bases of morphology in tomato varieties exhibiting elongated fruit shape. *Theor Appl Genet* 116:647–656. <https://doi.org/10.1007/s00122-007-0698-7>
- Gupta K, Chou MY, Howell A et al (2007) Cranberry products inhibit adherence of P-fimbriated *Escherichia Coli* to primary cultured bladder and vaginal epithelial cells. *J Urol* 177:2357–2360. <https://doi.org/10.1016/j.juro.2007.01.114>
- Hagidimitriou M, Roper T (1994) Seasonal changes in nonstructural carbohydrates in cranberry. *J Am Soc Hortic Sci* 119:1029–1033
- Harker FR, Marsh KB, Young H et al (2002) Sensory interpretation of instrumental measurements 2: sweet and acid taste of apple fruit. *Postharvest Biol Technol* 24:241–250. [https://doi.org/10.1016/S0925-5214\(01\)00157-0](https://doi.org/10.1016/S0925-5214(01)00157-0)
- Honda C, Kotoda N, Wada M et al (2002) Anthocyanin biosynthetic genes are coordinately expressed during red coloration in apple skin. *Plant Physiol Biochem* 40:955–962. [https://doi.org/10.1016/S0981-9428\(02\)01454-7](https://doi.org/10.1016/S0981-9428(02)01454-7)
- Houle D, Govindaraju DR, Omholt S (2010) Phenomics: the next challenge. *Nat Rev Genet* 11:855–866
- Jaakola L (2002) Expression of genes involved in anthocyanin biosynthesis in relation to anthocyanin, proanthocyanidin, and flavonol levels during bilberry fruit development. *Plant Physiol* 130:729–739. <https://doi.org/10.1104/pp.006957>
- Jayasena V, Cameron I (2008) Brix/acid ratio as a predictor of consumer acceptability of crimson seedless table grapes. *J Food Qual* 31:736–750. <https://doi.org/10.1111/j.1745-4557.2008.00231.x>

- Jesse E, Saupé W, Deller S, Lohr R, Roper T, Stang E (1993) The economic impact of the Wisconsin cranberry industry. The Cranberry Institute, East Wareham, MA
- Kaczmarek E (2009) Growth, flowering and yielding of six American cranberry (*Vaccinium macrocarpon* Ait.) cultivars. *Acta Sci Pol Hortorum Cult* 8:35–44
- Lacroix DS (1926) Cranberry flower-bud investigations. *J Agric Res* 33:355–363
- Liu H, Liu H, Wang W et al (2011) Cranberry phytochemicals inhibit glycation of human hemoglobin and serum albumin by scavenging reactive carbonyls. *Food Funct* 2:475–482. <https://doi.org/10.1039/c1fo10087d>
- Marwan AG, Nagel CW (1986) Microbial inhibitors of cranberries. *J Food Sci* 51:1009–1013. <https://doi.org/10.1111/j.1365-2621.1986.tb11220.x>
- McCown BH, Zeldin EL (2003) “HyRed”, an early, high fruit color cranberry hybrid. *HortScience* 38:304–305
- Nogales-Bueno J, Baca-Bocanegra B, Rodríguez-Pulido FJ et al (2015) Use of near infrared hyperspectral tools for the screening of extractable polyphenols in red grape skins. *Food Chem* 172:559–564. <https://doi.org/10.1016/j.foodchem.2014.09.112>
- Pappas E, Schaich KM (2009) Phytochemicals of cranberries and cranberry products: Characterization, potential health effects, and processing stability. *Crit Rev Food Sci Nutr* 49:741–781. <https://doi.org/10.1080/10408390802145377>
- Pierre JF, Heneghan AF, Feliciano RP et al (2013) Cranberry proanthocyanidins improve the gut mucous layer morphology and function in mice receiving elemental enteral nutrition. *J Parenter Enter Nutr* 37:401–409. <https://doi.org/10.1177/0148607112463076>
- Polashock J, Zelzion E, Fajardo D et al (2014) The American cranberry: First insights into the whole genome of a species adapted to bog habitat. *BMC Plant Biol*. <https://doi.org/10.1186/1471-2229-14-165>
- Roper TR, Stang EJ, Hawker GM (1992) Early season leaf removal reduces fruit set and size in cranberry (*Vaccinium macrocarpon* Ait.). *HortScience* 27:75–75
- Roper TR, Patten KD, DeMoranville CJ et al (1993) Fruiting of cranberry uprights reduces fruiting the following year. *HortScience* 28:228–228
- Schlautman B, Covarrubias-Pazarán G, Diaz-García LA et al (2015) Development of a high-density cranberry SSR linkage map for comparative genetic analysis and trait detection. *Mol Breed*. <https://doi.org/10.1007/s11032-015-0367-5>
- Schlautman B, Covarrubias-Pazarán G, Diaz-García L et al (2017) Construction of a high-density American Cranberry (*Vaccinium macrocarpon* Ait.) composite map using genotyping-by-sequencing for multi-pedigree linkage mapping. *G3 Gene Genom Genet* 7:1177–1189. <https://doi.org/10.1534/g3.116.037556>
- Shabrova EV, Tarnopolsky O, Singh AP et al (2011) Insights into the molecular mechanisms of the anti-atherogenic actions of flavonoids in normal and obese mice. *PLoS One*. <https://doi.org/10.1371/journal.pone.0024634>
- Su X, Howell AB, D’Souza DH (2010) Antiviral effects of cranberry juice and cranberry proanthocyanidins on foodborne viral surrogates—a time dependence study in vitro. *Food Microbiol* 27:985–991. <https://doi.org/10.1016/j.fm.2010.05.027>
- Taghadomi-Saberi S, Omid M, Emam-Djomeh Z, Ahmadi H (2014) Evaluating the potential of artificial neural network and neuro-fuzzy techniques for estimating antioxidant activity and anthocyanin content of sweet cherry during ripening by using image processing. *J Sci Food Agric* 94:95–101. <https://doi.org/10.1002/jsfa.6202>
- Vanden Heuvel JE, Davenport JR (2005) Effects of light, temperature, defoliation, and fruiting on carbon assimilation and partitioning in potted cranberry. *HortScience* 40:1699–1704
- Vorsa N, Johnson-Cicalese J (2012) American cranberry. In: Badenes ML, Byrne DH (eds) *Fruit breeding*. Springer, Boston, pp 191–223
- Vorsa N, Polashock J (2000) Evaluation of fruit chemistry in cranberry germplasm: potential for breeding varieties with enhanced health constituents. *Acta Hort* 574:215–219. <https://doi.org/10.17660/ActaHortic.2002.574.32>
- Vorsa N, Polashock J (2005) Alteration of anthocyanin glycosylation in cranberry through interspecific hybridization. *J Am Soc Hortic Sci* 130:711–715
- Vvedenskaya IO, Vorsa N (2004) Flavonoid composition over fruit development and maturation in American cranberry, *Vaccinium macrocarpon* Ait. *Plant Sci* 167:1043–1054. <https://doi.org/10.1016/j.plantsci.2004.06.001>
- Wang Y, Johnson-Cicalese J, Singh AP, Vorsa N (2017) Characterization and quantification of flavonoids and organic acids over fruit development in American cranberry (*Vaccinium macrocarpon*) cultivars using HPLC and APCI-MS/MS. *Plant Sci* 262:91–102. <https://doi.org/10.1016/j.plantsci.2017.06.004>
- Xiao H, Radovich C, Welty N et al (2009) Integration of tomato reproductive developmental landmarks and expression profiles, and the effect of SUN on fruit shape. *BMC Plant Biol* 9:49. <https://doi.org/10.1186/1471-2229-9-49>
- Xu TY, Sun J, Chang HL et al (2017) QTL mapping for anthocyanin and proanthocyanidin content in red rice. *Euphytica* 213:243
- Yoshioka Y, Nakayama M, Noguchi Y, Horie H (2013) Use of image analysis to estimate anthocyanin and UV-excited fluorescent phenolic compound levels in strawberry fruit. *Breed Sci* 63:211–217. <https://doi.org/10.1270/jsbbs.63.211>